Journal of
Mechanical
Science and
Technology

Journal of Mechanical Science and Technology 21 (2007) 415~420

Analytical and Experimental Study of Mismatch Strain-Induced Microcantilever Behavior during Deposition

Sang-Hyun Kim[a,*], James G. Boyd IV[b]

[a]*Micro Device & Systems Lab., Samsung Advanced Institute of Technology, Mt. 14-1, Nongseo-dong, Giheung-gu, Younggin-si, Gyunggi-do, 449-712, Korea,*
[b]*Department of Aerospace Engineering, 3141 TAMU, Texas A&M University, College Station, TX, 77843-3141, USA*

(Manuscript Received August 4, 2006; Revised January 13, 2007; Accepted January 14, 2007)

Abstract

A model of mechanical behavior of microcantilever due to mismatch strain during deposition of MEMS structures is analytically derived and experimentally verified. First, a microcantilever, modeled as an Euler-Bernoulli beam, is subjected to deposition of another material and a linear ordinary differential equation which considers the through-thickness variation of the mismatch strain is derived. Second, the deposition analysis is experimentally verified by electroplating of nickel onto an AFM cantilever beam. The deflection of the AFM cantilever is measured in-situ as a function of the deposited thin film thickness through the optical method of Atomic Force Microscopy and the mismatch strain with the through-thickness variation is determined from the experiment results. The usefulness of these equations is that they are indicative of the real time behavior of the structures, i.e. it predicts the deflection of the beam continuously during deposition process.

Keywords: Multilayer microcantilever; Atomic force microscope; Mismatch strain; Nickel electroplating; Beam deflection

1. Introduction

Micromachined multilayer cantilevers have been widely used in microelectronics, optical and structural components (Tien et al., 1996; Kiang et al., 1996). The mechanical response of multilayer cantilevers is affected by residual stresses, which are generated from the fabrication process such as physical or chemical vapor deposition, sputtering and electro-plating. Due to the mismatch between the deposited film and the substrate, a residual stress is generated, which subsequently causes a deformation in the cantilever (Madow, 1993). Thus, residual stresses usually have deleterious effects in thin film processing, such as film buckling, warping, blistering, cracking, delamination and void formation.

There have been a few attempts to develop useful applications of residual stresses in MEMS. This work dates to the Stoney formula (Stoney, 1909) for the curvature of thin films on a thick substrate. Freund (1996) proposed a theory that predicted the response of thin films to mismatch strain produced during the film growth. This was an improvement over the Stoney formula, as it eschewed the assumption that the deposited layer is very thin compared to the thin-film substrate. Prinz et al. (2001) used residual stresses to make cylindrical nano structures. A laminate consisting of B doped Si, undoped Si, B doped Si, Ge, and B doped Si was deposited with no curvature. The undoped Si layer was etched away, allowing the upper three layers (b doped Si, Ge, B doped Si) to deform (or "roll up") into cylinders with radii of curvature from 0.3 to 2 micrometers. How-

*Corresponding author. Tel.: +82 31 280 8146
E-mail address: shkim004@gmail.com

ever, it is not suitable to predict the real time behavior of the structure during deposition process. In order not to use the trials and errors it is desirable to be able to predict the final shape of multilayer microcantilevers due to the residual stresses, especially the intrinsic stress. An analysis has recently been performed to study the mechanics of using residual stress changes and to predict the real time behavior of the structure during deposition process (Kim et al., 2006). However, they did not consider the through-thickness (out-of-plane) variation of the mismatch strain, which should be measured by experiment for more accurate prediction of the mismatch strain-induced beam deflection during deposition process.

This research presents a model of mechanical behavior of microcantilever due to mismatch strain during deposition of MEMS structures. First, a microcantilever, modeled as an Euler-Bernoulli beam, is subjected to deposition of another material and a linear ordinary differential equation whose mismatch strain varies during deposition was derived as a function of the deposited layer thickness. Second, the deposition analysis is experimentally verified by electroplating of nickel onto an AFM cantilever beam. The deflection of the AFM cantilever is measured in-situ as a function of the deposited thin film thickness through the optical method of AFM and the mismatch strain with the through-thickness variation is determined from the experiment results.

2. Theoretical modeling

The prismatic beam has constant length L, constant width b, and variable thickness h. The substrate with Young's modulus of E_1 is designated as region 1 and has a constant thickness h_1. The deposited material with Young's modulus of E_2 has a variable thickness h_2, and $h = h_1 + h_2$. The schematic of the microcantilever is shown in Fig. 1. Material is then deposited on the surface $y = h\ (h \geq h_1)$,

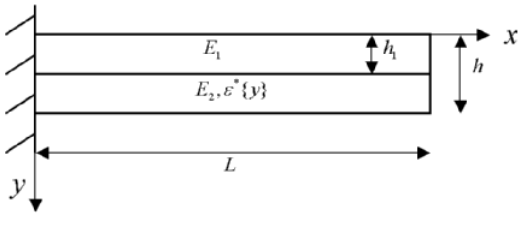

Fig. 1. Schematic of the microcantilever.

which causes the beam to bend, depending on the sign of the mismatch strain in the deposited material. Kim et al. (2006) derived the ordinary linear differential equation for the end-deflection $v\{h\}$ of the microcantilever as a function of the deposited layer thickness h when the reference mismatch strain ε^* is constant and ex-pressed as

$$\frac{dv\{L;h\}}{dh} = -3\varepsilon^* \frac{g\{h\}}{f\{h\}} L^2 \tag{1}$$

where

$$f\{h\} = \left(h + (\bar{E}-1)h_1\right)^{-1}\left(-h^4 - 4h^3 h_1(\bar{E}-1)\cdot \right.$$
$$\left. + 6h^2 h_1^2(\bar{E}-1) - 4hh_1^3(\bar{E}-1) - h_1^4(\bar{E}-1)^2\right)$$
$$g\{h\} = \left(h + (\bar{E}-1)h_1\right)^{-1}\left(h^2 + 2hh_1(\bar{E}-1) - h_1^2(\bar{E}-1)\right)$$

and $\bar{E} = E_1 / E_2$

The mismatch strain is due to growth processes or lattice mismatch between the deposited material and the deposited surface and the reference value $\varepsilon^*\{y\}$ of the mismatch strain is the mismatch strain that results from deposition on a strain-free substrate; for example, a flat substrate that is free of stress. $\varepsilon^*\{y\}$ at a given y does not change in time, so $d\varepsilon^* = 0$. Considering the through-thickness variation of the mismatch strain during deposition, Eq. (1) can be modified as

$$\frac{dv\{L;h\}}{dh} = -3\,\varepsilon^*\{y\}\Big|_{y=h} \frac{g\{h\}}{f\{h\}} L^2 \tag{2}$$

In order to numerically solve Eq. (2), the reference mismatch strain $\varepsilon^*\{y\}$ at $y = h$ must be known. The reference mismatch strain will be determined by interpreting experimental results in terms of the relation between the cantilever curvature and the mismatch strain. The mismatch strain is simply expressed by

$$\varepsilon^m\{y\} = \varepsilon^*\{y\} + y\kappa\{x;y\} - \varepsilon^r\{y\} \tag{3}$$

where $\kappa\{x;y\}$ is the curvature about the z axis and $\varepsilon^r\{y\}$ is the strain of the reference layer, $y = 0$. Freund (1996) proposed the connections between the cantilever curvature and the mismatch strain for the

homogeneous case $(E_1 = E_2)$. Referring to the results of Freund (1996), the curvature and the reference strain are expressed in the term of the mismatch strain for the inhomogeneous case,

$$\kappa\{x;h\} = -\frac{6}{h^2}\frac{A\{h\}}{D\{h\}}\int_0^h \varepsilon^m\{y\}dy + \frac{12}{h^3}\frac{B\{h\}}{D\{h\}}\int_0^h y\varepsilon^m\{y\}dy \quad (4)$$

$$\varepsilon^r\{x;h\} = -\frac{4}{h}\frac{C\{h\}}{D\{h\}}\int_0^h \varepsilon^m\{y\}dy + \frac{6}{h^2}\frac{A\{h\}}{D\{h\}}\int_0^h y\varepsilon^m\{y\}dy \quad (5)$$

where,

$$A\{h\} = \frac{h_1^2}{h^2}(\bar{E}-1)+1, B\{h\} = \frac{h_1}{h}(\bar{E}-1)+1,$$

$$C\{h\} = \frac{h_1^3}{h^3}(\bar{E}-1)+1,$$

$$D\{h\} = 4\left[\frac{h_1}{h}(\bar{E}-1)+1\right]\left[\frac{h_1^3}{h^3}(\bar{E}-1)+1\right] - 3\left[\frac{h_1^2}{h^2}(\bar{E}-1)+1\right]^2$$

Substituting Eqs. (4) and (5) into Eq. (3) yields:

$$\varepsilon^*\{y\} = \varepsilon^m\{y\} - \frac{2}{yD\{y\}}\left[2C\{y\}-3A\{y\}\right]\int_0^y \varepsilon^m\{y\}dy - \frac{6}{y^2D\{y\}}\left[2B\{y\}-A\{y\}\right]\int_0^y y\varepsilon^m\{y\}dy \quad (6)$$

Therefore, the reference mismatch strain $\varepsilon^*\{y\}$ can be determined if the mismatch strain $\varepsilon^m\{y\}$ is obtained. This mismatch strain can be obtained through the experiment results.

In the experiment, one would measure the end beam deflection $v\{L;h\}$ of cantilever as a function of the deposited layer thickness h. The cantilever curvature is expressed by the second derivative of the deflection $v\{x;h\}$. Assume the deposited layer is applied in a manner that is not a function of x, the curvature is expressed by

$$\kappa\{h\} = \frac{2v\{L;h\}}{L^2} \quad (7)$$

From Eq. (7), for each value of h, the curvature can be experimentally obtained from the end beam deflection. The through-thickness variation of the mismatch strain $\varepsilon^m\{y\}$ can be approximated as a polynomial function of y and the unknown parameters of the polynomial function can be determined from Eq. (4). Finally the reference mismatch strain $\varepsilon^*\{y\}$ can be determined from Eq. (6).

3. Experimental description

The goal of the experiment is to physically realize the device of Fig. 1 and to measure the reference mismatch strain for solving Eq. (2), which determined from the measurement of the deposited layer thickness and the end beam deflection. In order to measure the cantilever deflection as a function of the deposited layer thickness, a commercial AFM (Nanoscope IIIA of Digital Instruments) is used. An insoluble nickel electroplating is selected as the deposition process. Experiment set-up consists of the AFM cantilever ($NSC16/Si_3N_4$: MikroMasch), insoluble positive electrode (platinum wire, model CHI115: CH Instruments, Inc.), electrochemical fluid cell and power supply. An all-sulfate nickel solution is used to keep the consistent nickel concentration in the fluid cell during deposition process, which consists of the nickel sulfate (225~400 g/l) and boric acid (30~45 g/l)(Schlesinger, 2000). The current is applied via a power supply between the AFM cantilever (working electrode) and the platinum wire (counter electrode). Fig. 2 shows the schematic drawing of the experiment set-up. Material is electro-plated onto the AFM cantilever, which produces residual stresses that deform the beam. The electro-plated AFM cantilever serves as the sensing can-tilever because its end deflection is measured on the top surface using an optical method of AFM. The cantilever deflection is monitored through a change in the slope of the cantilever at the position of the photodetector. The beams are supplied with a 10 nm silicon nitride passivation layer applied to both sides of the beams. A Cr/Au layer is then evaporated onto the tip surface of the deposition beam to provide electrical conductivity for subsequent electroplating of nickel. The current density for this plating is recommended to be limited in the range of 20~100 mA/cm^2. The platinum counter electrode has the area of 7.85×10^{-2} cm^2, therefore, the input current of the power supply is set to 4 mA, which makes the current density in the recommended range (J=51 mA/cm^2). To avoid the

bending of the cantilever due to temperature change all experiments are kept at the room temperature.

Thin layers of nickel are electroplated onto the tip surface of AFM cantilever and their thicknesses are measured using DEKTAK[3], a commercial surface profile measuring system, at the center and two side edges of each AFM cantilever to check the thickness uniformity of the cantilever. Generally the surface profiler requires the presence of a groove or a step between the substrate and film surface such that the stylus is vertically displaced as it traverses the sample. Hence, the gold layer is initially coated on the portion of the AFM cantilever and the nickel is deposited only on the portion of the AFM cantilever during electroplating and makes a step between the plated and unplated layers. The Young's modulus of electroplated nickel varies greatly depending on the processing conditions (Sharpe, 2002) and can be determined from the resonance method of AFM, by measuring the change of the resonant frequency due to the mass change of electroplated AFM cantilever.

The beam deflection can not be measured directly as a function of the deposited layer thickness during electroplating. Instead, the nickel plating rate is measured for the given experimental parameters by plating in a series of steps and using the profilometer to measure the nickel thickness after each step. Then the deflection of the deposition beam is measured as a function of time. Since both the deflection and the deposition thickness are known functions of time, it is possible to express the beam deflection as a function of the deposited film thickness. The deflections can then be converted into curvatures using Eq. (7).

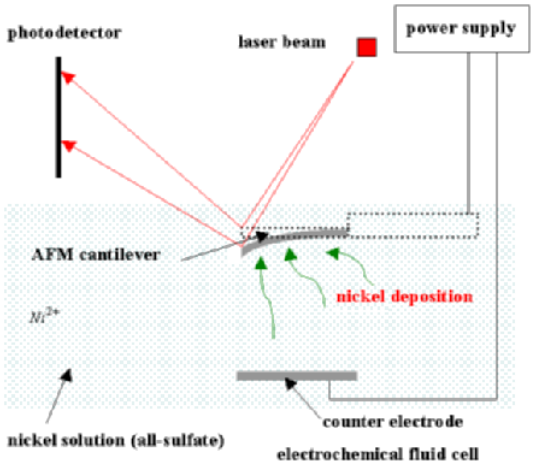

Fig. 2. Schematic drawing of experimental set-up.

Finally, the reference mismatch strain as a function of the out-of-plane coordinate (y) is calculated using Eq. (6).

4. Results and discussion

Five different samples of AFM cantilevers were chosen for plating and sample cantilever was loaded in the electrochemical cell of AFM each by each and thin layers of Ni were electroplated onto the surface of the sample cantilever during the five fifteen second plating steps. After each plating step, we measured the plating thickness of each sample cantilever using a surface profiler at three different positions (center and two side edges of the groove). The variations of the measured plating thicknesses were less than 4.3 %. Fig. 3 gives the total plated nickel thickness of each cantilever during plating step. The total thickness of plated nickel was increased as increasing the plating time. The plating rate of each cantilever should be identical but they were different, which might come from the errors of the thickness measurement and the allowed plating time to each cantilever. Obviously the plating time is not the pertinent parameter for the analysis because the measured resonant frequency and Young's modulus are highly dependent of the plating thickness. Therefore, the difference of the plating thickness of sample cantilevers with equal plating duration is meaningless.

Young's modulus of the electroplated Ni was determined by using the measured resonant frequencies and the plated Ni thickness of each cantilever at the end of each plating step. Fig. 4 presents the evolution of Young's modulus of the electroplated Ni films with the plated nickel thickness. The measured values of Young's modulus of each cantilever ranged from 148.04 GPa to 159.90 GPa. The total average Young's

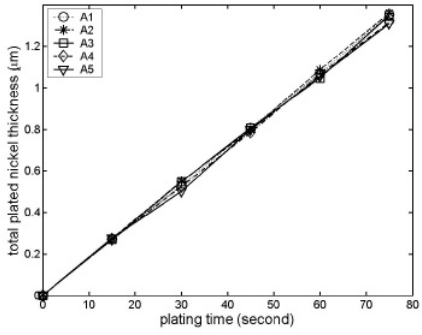

Fig. 3. Total plated nickel thickness of each cantilever during plating step.

modulus of electroplated Ni film is 155.36 GPa with the maximum standard deviation of 3.47. These values are smaller than that of the bulk Ni (207 Gpa) but relatively closed to those values for thin Ni films (Sharpe, 2002).

The end deflections of each cantilever at the end of each plating step are shown in Fig. 5. Amount of deflection of each cantilever was different due to the difference of AFM sample cantilever stiffness. The rate of deflection with plating time of each cantilever was decreasing, which agrees with other experimental results (Wang, 2005).

In order to determine the reference mismatch strain, the beam deflections were determined as a function of plating thickness, and then converted into curvatures using Eq. (7). Finally, the reference mismatch strain as a function of the out-of-plane coordinate was calculated for five beams, and the average response is shown in Fig. 6. This analytical result indicates that the reference mismatch strain is decreasing in the out-of plane direction, which is similar to the other experiment results (Wang, 2005).

The end deflection of the cantilever was analytically solved by using Eq. (2) and the calculated reference mismatch strain. Fig. 7 shows the comparison of the beam deflection during deposition when the reference mismatch strain is and is not a function of the out of plane location. The solid line indicates the model results when the reference mismatch strain does not vary through the thickness. These results differ greatly from the real case in which the reference mismatch strain varies.

5. Conclusions

In this paper, a model of mechanical behavior of microcantilever due to mismatch strain during deposition of MEMS structures was investigated. A linear ordinary differential equation whose mismatch strain varies during deposition was derived as a function of the deposited layer thickness. Because the mismatch strain highly depends on the deposition materials and

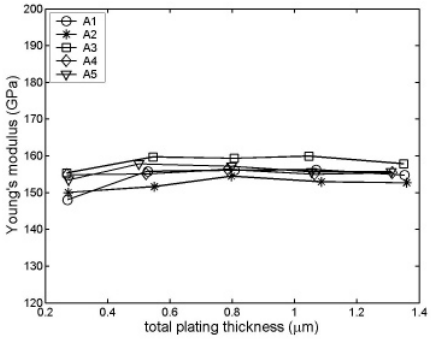

Fig. 4. Evolution of Young's modulus of electroplated Ni thin films.

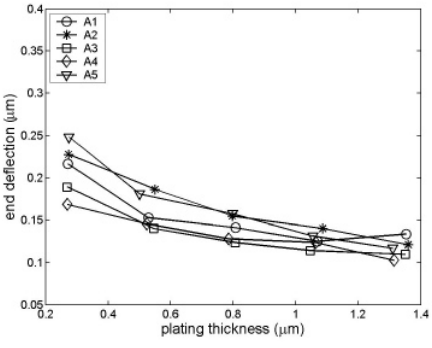

Fig. 5. End deflections of each cantilever at the end of each plating step.

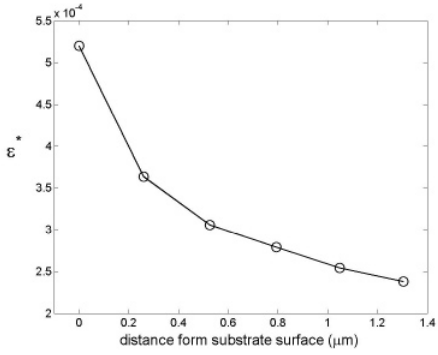

Fig. 6. Calculated reference mismatch strain vs out-of-plane location.

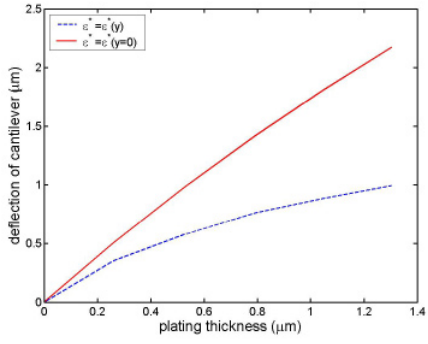

Fig. 7. Comparison of the beam deflection during deposition when the reference mismatch strain is and is not a function of the out-of plane location.

the processes, the equation can only be solved after the mismatch strain is determined through the experiment, by measuring the deposited layer thickness and the cantilever curvature. It is the only drawback of this approach. However, current MEMS companies have high quality facilities and fabrication recipe, therefore, the database of the mismatch strain during diverse deposition materials and processes enables predict the real time behavior of the structures Deposition analysis is experimentally verified by electroplating of nickel onto an AFM cantilever beam. Electroplated Ni is selected for the plating material because it has become a commonly used material as mechanical structures in MEMS and its plating solution are well defined. AFM cantilever beam was working as a sensing cantilever, which did not require the microfabricated sensing cantilever and additional experiment setup to measure the beam deflection. The measured deflection rate and the determined reference mismatch strain well agree with other experiment results.

References

Chang, C., Chang, P., 2000, "Innovative Micromachined Microswitch with Very Low Insertion Loss," *Sensors and Actuators*, Vol. A79, pp. 71~75.

Freund, L. B., 1996, "Some Elementary Connections Between Curvature and Mismatch Strain in Compositionally Graded thin Films," *Journal of the Mechanics and Physics of Solids,* **44** pp. 723~736.

Kiang, M. H., Solgaard, O., Muller, R. S., Lau, K. Y., 1996, "Silicon-Micromachined Micromirrors with Integral High-Precision Actuators for External-Cavity Semi-Conductor Laser," *IEEE Photonics Technology Letters*, Vol. 8, pp. 95~97.

Kim, S. -H., Boyd, J. G., 2006, "Modeling of Mechanical Behavior of Microcantilever Due to Intrinsic Strain During Deposition," *Accepted for Publishing in the Journal of Mechanical Science and Technology*, Vol. 20, No. 10., pp. 0~0.

Madou, M., 1993, *Fundamentals of Microfabrication*, Boca Raton: CRC Press, LLC.

Prinz, V. Y., Grutzmacher, D., Beyer, A., David, C., Ketterer, B., Deckardt, E., 2001, "A New Technique for Fabricating Three-Dimensional Micro-and Nanostructures of Various Shapes," *Nanotechnology*, vol. 12, pp. 399~ 402.

Schlesinger, M., Paunovic, M., 2000, "Modern Electroplating," John Wiley & Sons.

Sharpe W. N., 2002 *MEMS Handbook: Chapter 3 – Mechanical Properties of MEMS Material* (Boca Raton: CRC Press).

Tien, N. C., Solgaard, O., Kiang, M-H., Daneman, M., Lau, K. Y., Muller, R. S., 1996, "Surface-Micromachined Mirrors for Laser-Beam Positioning," *Sensors and Actuators*, Vol. A52, pp. 76~80.

Wang Y., Ballarini R., Kahn H., Heuer A. H., 2005, "Determination of The Growth Strain of LPCVD Polysilicon," *Journal of Microelectromechanical Systems* **14** pp. 160~166.